THE STRUCTURAL AND BIOCHEMICAL CHARACTERIZATION OF DEUBIQUITINATING ENZYMES LOTA AND UCHL1 R178Q

by

Kwame J. Brown

A Thesis

Submitted to the Faculty of Purdue University

In Partial Fulfillment of the Requirements for the degree of

Master of Science

Department of Chemistry

West Lafayette, Indiana

August 2019

THE PURDUE UNIVERSITY GRADUATE SCHOOL
STATEMENT OF COMMITTEE APPROVAL

Dr. Chittaranjan Das, Chair

Department of Chemistry

Dr. Mathew Tantama

Department of Chemistry

Dr. Nicholas Noinaj

Department of Biological Sciences

Approved by:

Dr. Christine Hrycyna

Head of the Graduate Program

ACKNOWLEDGMENTS

I would like to acknowledge the entire Das lab. Kedar, Kristos, Kenny, Zhengrui, and Shalini. You have all been amazing and I wish you all continued success. I appreciate all the support during my time in the lab. It means the most to me. I also acknowledge my undergrads Rachel Hohe and Ashley Zeese. Thank you for your patience and wish you both well on your journeys. I also would like to thank John Hausman for support and experiences during his time in the Das lab. I would like to thank my committee and Dr. Das. Last but not least I would like to thank my family and loved ones. I can’t wait to come home.

TABLE OF CONTENTS

LIST OF TABLES 6
LIST OF FIGURES 7
LIST OF ABBREVIATIONS 8
ABSTRACT 9
CHAPTER 1. INTRODUCTION 10
1.1 Ubiquitin 10
1.2 Deubiquitinating Enzymes 10
1.3 *Legionella* effector LotA 11
1.4 UCHL1 R178Q 12
CHAPTER 2. EXPERIMENTAL 14
2.1 LotA Cloning, Expression, and Purification 14
2.2 Enzymatic Preparation of K6 Di-Ubiquitin 14
2.3 Purification of Ub-MESNa for Ub-Prg reaction 15
2.3.1 Reaction with Propargylamine 15
2.4 LotA Primer design and Cloning 16
2.5 UCHL1 R178Q Expression and Purification 16
2.5.1 Primer Design of UCHL1 mutants 17
2.6 Protein Crystallization and Structure Determination UCHL1 R178Q 17
2.6.1 Novel Protein Crystallization technique for WT UCHL1 18
2.7 Enzymatic Activity Assay for UCHL1 Mutants 18
2.8 Circular Dichroism of WT UCHL1 and R178Q 19
CHAPTER 3. RESULTS AND DISCUSSION: LOTA 20
3.1 Investigations into LotA First Catalytic Domain 20
3.1.1 Expression and Purification $LotA_{1-290}$ 21
3.1.2 Preparation of K6-Ub_2 22
3.1.3 Specificity Assay for $LotA_{1-290}$ 23
3.1.4 $LotA_{1-290}$ Kinetic Profile 24
3.1.5 Activity Probe Shift Assay 26

3.2 Further Insight into LotA; Identification of Distal Site Interacting Residues of Domain 1 27
3.3 Expression and Activity of LotA Second Catalytic Domain 30
CHAPTER 4. RESULTS AND DISCUSSION UCHL1 R178Q 33
4.1 Structural Insight into UCHL1 R178Q 33
4.2 Biochemical Analysis 38
4.2.1 Kinetic Profile WT UCHL1 vs R178Q 39
4.3 Stability Analysis 40
4.4 Further Discussions 41
CHAPTER 5. CONCLUSION 44
5.1 LotA 44
5.2 UCHL1 R178Q 45
REFERENCES 46

LIST OF TABLES

Table 3.1Kinetic Parameters LotA$_{1-290}$ 26
Table 4.1 Kinetic ParametersUCHL1 WT and R178Q 40

LIST OF FIGURES

Figure 3.1. Domain diagram of LotA. 20

Figure 3.2. Purification gel of $LotA_{1-290}$. 21

Figure 3.3 Chromatogram of $LotA_{1-290}$ SEC..... 22

Figure 3.4 Ion exchange Mono S chromatogram for K6-Ub_2 reaction product. 23

Figure 3.5 SDS PAGE gel of Mono S fraction for K6-Ub_2 reaction..... 23

Figure 3.6 Specificity assay for $LotA_{1-290}$ (left) and time dependent assay (right)..... 24

Figure 3.7 Plot of $LotA_{1-290}$ kinetic experiment..... 25

Figure 3.8 Fitting of Michaelis-Menten data. 26

Figure 3.9 Comparison of Activity based probe shift assay; Ub-Pa (left), Ub-VME (right). 27

Figure 3.10 $LotA_{1-252}$ cleavage assay at E:S concentrations 4 and 35uM respectively. 28

Figure 3.11 $LotA_{1-269}$ Ub-Pa shift assay. 29

Figure 3.12 LotA $_{1-252}$ and $LotA_{1-259}$ activity shift assay. 29

Figure 3.13 SDS PAGE gel of $LotA_{293-613}$ Purification..... 31

Figure 3.14 The Ub-Pa shift assay with $LotA_{293-613}$. This construct is unreactive on its own..... 32

Figure 4.1 Purification gel of UCHL1 R178Q..... 34

Figure 4.2 Chromatogram of S75 SEC purification of UCHL1 R178Q..... 34

Figure 4.3 SDS-PAGE gel of SEC fractions for UCHL1 R178Q. Fractions C5 and onward were used for further studies. 35

Figure 4.4 UCHL1 R178Q crystals from C4 condition..... 35

Figure 4.5 Electron density map UCHL1 R178Q. Density is shown for H161 and Q178..... 36

Figure 4.6 The distance of H161 and C90 for the UCHL1 R178Q structure. 37

Figure 4.7 Residue E60 forming close interaction with H161 of R178Q crystal structure..... 38

Figure 4.8 Ub-Rho activity assay on UCHL1 WT and mutants..... 39

Figure 4.9 Kinetic profiles of UCHL1 WT and R178Q. 40

Figure 4.10 CD thermal melt of UCHL1 WT and R178Q. 41

Figure 4.11 UCHL1 R178Q existing as dimer in crystal structure..... 43

Figure 4.12 Comparison of SEC (S75) chromatograms for WT (left) and mutant R178Q (right). The splitting of the major peak is opposite for the two proteins..... 43

LIST OF ABBREVIATIONS

DUB	Deubiquitinating
Ub	Ubiquitin
Ub-Pa	Ubiquitin Propargylamide
IPTG	Isopropyl β-D-1- thiogalactopyranoside
WT	Wild Type
VME	Vinyl Methyl Ester
ATP	Adenosine triphosphate
GST	Glutathione S Transferase
DTT	Dithiothreitol
SEC	Size exclusion chromotagraphy
SDS	Sodium dodecyl sulfate

ABSTRACT

Author: Brown, Kwame, J. MS
Institution: Purdue University
Degree Received: August 2019
Title: The Structural and Biochemical Characterization of Deubiquitinating Enzymes LotA and UCHL1 R178Q
Committee Chair: Chittaranjan Das

The Deubiquitinating (DUB) enzymes, LotA and UCHL1 R178Q, were examined biochemically and also structurally in the case of UCHL1 R178Q. LotA is a bacterial effector of *Legionella pneumophila* that enables the pathogen to establish a replicative niche. LotA has two Deubiquitinase (DUB) domains specific to different substrates. Here, I report biochemical examinations the first DUB domain that is specific to Lys6-linked di-ubiquitin. Michaelis-Menten kinetic parameters were determined for this domain. Through activity assays of various truncations a series of residues were discerned that contribute to interaction of the distal binding site of ubiquitin chain.

UCHL1 mutant R178Q displays enhanced activity when compared to wild type (WT). The mutant was crystallized for structural analysis to gain insights into the higher catalytic activity of the mutant. The structure revealed that the catalytic histidine maintains a misaligned orientation similar to the WT enzyme. Biochemical analysis was done to ascertain the role of key residues that interact with the catalytic histidine. The residue type at position 178 in the structure plays a key role in enhancing the enzyme activity.

CHAPTER 1. INTRODUCTION

1.1 Ubiquitin

Ubiquitin is a small protein consisting of 76 amino acids with a molecular weight of approximately 8.5 kDa with a characteristic beta grasp fold [1]. Ubiquitin mainly serves as a signaling molecule for post-translational modification. The post-translational modification ubiquitination plays a crucial role in eukaryotic organisms. The attachment of ubiquitin to a target protein is achieved via covalent formation of an isopeptide bond through the enzymatic action of a trio of enzymes (E1, E2, E3)[1]. The E1 enzyme is considered the activating enzyme, which utilizes adenosine triphosphate (ATP) for the formation of a reactive thioester bond with ubiquitin [2]. This activated ubiquitin is then transferred to an E2 enzyme, called conjugating enzyme [1]. Ubiquitin is then transferred from the E2 enzyme to an E3 enzyme termed ubiquitin ligase [1,2]. Through the action of the E3 enzyme ubiquitin is attached to Lysine residues of substrate proteins [1,2].

1.2 Deubiquitinating Enzymes

Proteins that have been ubiquitinated have one of several fates. One such fate is degradation by targeting to the 26S proteasome for maintenance of proteome homeostasis [1]. Ubiquitination also plays a role in innate immunity, transcriptional activation, cell growth, histone modification, and several biosignaling pathways [1-5]. The process of ubiquitination is reversible due to the action of deubiquitinating enzymes called DUBs [2]. DUBs are proteases that cleave the isopeptide bond of ubiquitinated proteins or chains of ubiquitin [2]. Human DUBs are grouped into seven families based on structural and sequence similarity [3]. The seven families of DUBs are the OTU (Ovarian tumor), Ubiquitin specific proteases (USP), Ubiquitin

C-terminal hydrolases (UCH), Machado-Josephin domain proteases (MJD), JAMM family, MINDY, and ZUFSP [3]. The JAMM family is the only metalloprotease of the deubiquitinating enzymes, where the others are cysteine proteases [2].

A growing number of bacterial DUBs have been discovered containing papain like folds [4]. These include ElaD (*Escherichia coli*), SseL (*Salmonella enterica*), Cdu1 and Cdu2 (*Chlamydia trachomatis*), and a few DUBs secreted by *Legionella pneumophila* [4].

1.3 *Legionella* effector LotA

The Gram-negative pathogenic bacterium, *Legionella pneumophila*, causes a severe form of pneumonia called Legionnaires' disease. After entry into eukaryotic host cell, the bacterium creates a special vacuole to replicate in [4]. In creating the replicative niche, the bacterium utilizes a Type 4 secretion system where hundreds of effector proteins are released into host cytoplasm [4]. Among the *Legionella* effectors, has been the discovery of several DUBs [4-6], the first being an enzyme called SdeA [5]. Qiu *et al*. showed SdeA has a ligase and DUB domain [6]. SdeA was shown to perform ubiquitination independent of E1 and E2 enzymes diverging from the canonical ubiquitination cascade [6]. Sheedlo *et al*. presented a crystal structure of the DUB domain of SdeA, both apo and in complex with ubiquitin, along with biochemical data showing specificity towards K63 chain types [5].

The three other known DUBs discovered from *Legionella* are LotA, LupA, and the more recent discovery, RavD [4,7,8]. The work reported here focuses on the biochemical analysis of LotA. LotA has two catalytic cysteines (C13 and C303) with C303 being linked to the cleavage of ubiquitin from *Legionella* containing vacuoles (LCV) [4]. LotA is a 744 residue long protein containing three domains [4]. One of the catalytic cysteines is reported to be specific for K6 linked ubiquitin chains (C13); the other catalytic cysteine has preference for long K63 linked

ubiquitin chains [4]. LotA has homology to a human DUB of the OTU, members of which are shown to have strict linkage specificity for ubiquitin substrate chain types [4,9]. A di-ubiquitin cleavage assay and suicide substrate shift assay were employed to assess activity and the nature of specificity for LotA [4]. This was done on the first domain containing the first catalytic site. The construct length 1-290 was designed and expressed [4]. This construct allows for analysis of just the first catalytic site containing C13. Kubori *et al*. have shown that the catalytic cysteine, C303, was solely responsible for cleavage of long K63-linked ubiquitin chains by using inactive point mutation on residue C13 in their cleavage assay [4]. Residues 300-613 of LotA make up the second catalytic domain [4]. Residues 614-707 correspond to the PI(3)P lipid binding domain of LotA [4].

Three dimensional structure of LotA is yet unknown. The first catalytic domain of LotA was also kinetically uncharacterized when this work commenced. There was also very little evidence showing further activity profile for the second catalytic domain of LotA, highlighting that further biochemical analysis of LotA was needed and thus the aim of this work.

1.4 UCHL1 R178Q

The second DUB of interest for this work is UCHL1. UCHL1 is human DUB of 223 amino acids with high expression levels in the brain [10]. A mutant variant of UCHL1 (I93M) is linked to Parkinso's Disease [10]. UCHL1 is also linked to some cancers [11]. Das *et al*. crystallized wild type UCHL1 protein and determined its structure revealing a misaligned catalytic triad with the catalytic histidine nearly 9Å away from the catalytic cysteine [12]. Bourdreaux *et al*. crystallized wild type UCHL1 bound to ubiquitin vinyl methyl ester (VME) [13]. This substrate bound structure revealed significant conformational change, with the

catalytic histidine moving within optimal distance of the catalytic cysteine to enable normal cysteine protease catalysis mechanism [13].

A recent paper in Human Molecular Genetics shows a pair of UCHL1 variants implicated in early onset progressive neurodegeneration with optical atrophy [14]. It was noted that one of the UCHL1 variants (R178Q) possessed higher catalytic activity than wild type UCHL1 [14]. The mutant UCHL1 R178Q was approximately four fold more active than the wild type enzyme [14]. It was noted by Das *et al*. that R178 may stabilize the catalytic histidine in the misaligned position [12]. The R178Q mutation was linked to a protective effect against early onset progressive neurodegeneration with optical atrophy [14].

We sought to determine the mechanism of the enhanced catalytic activity of UCHL1 R178Q through structural analysis. I was able to crystalize the mutant to diffraction quality 2.8Å resolution. We observed in the electron density map that the catalytic histidine (H161) of the mutant has moved 1.7Å closer to the catalytic cysteine (C90) but still maintains a misaligned catalytic triad comparable to native enzyme. Michaelis-Menten kinetic analysis was conducted and showed larger values for both K_{cat} and K_m when compared to the wild type enzyme.

CHAPTER 2. EXPERIMENTAL

2.1 LotA Cloning, Expression, and Purification

The LotA construct 1-290 was sub cloned from *Legionella pneumophila* Philadelphia strain into vector pGex-6P-1. This was transformed into *Escherichia coli* BL-21 Codon Plus cells. Cultures were grown to an Optical Density (OD) of 0.4-0.6 at 37°C. Expression was induced with 300 uM Isopropyl β-D-1- thiogalactopyranoside (IPTG) and expressed at 18°C for 16-18 hours. The cells were lysed using French press and cleared via centrifugation at 100,000 x g for 1 hour at 4°C. The protein was purified in two-step process using standard GST affinity chromatography technique as described by GE Healthcare. The tag subtracted protein was further purified using size exclusion chromatography (Superdex 75). The eluted fractions were collected based on maximal peak height on the chromatogram.

2.2 Enzymatic Preparation of K6 Di-Ubiquitin

After a small scale pilot experiment for K6 di-ubiquitin preparation, a large scale preparation was conducted. For the large scale reaction an amount of 5mL of 2x Ligation buffer was prepared by mixing 400 uL of 1M Tris-HCl pH 7.5 with 81mg of Magnesium Chloride ($MgCl_2$) and 60.5mg of Adenosine triphosphate (ATP). A volume of 24uL of 1M DTT was included in the mixture which was vortexed to make a homogenous solution. The final concentration of this buffer solution was 80 mM Tris-HCl pH 7.5, 1.2 mM DTT, 20 mM $MgCl_2$, and 20 mM ATP. The enzymatic reaction required the addition 200 uL of E1 enzyme at approximately 100 uM to the ligation buffer followed by 200 uL each of both E2 (UbcH7) and E3 (NleL) enzymes at approximately 100 uM. About 200 μL each of the ubiquitin triple mutant Ub K6R K48R K63R, and ubiquitin double mutant, Ub K48R D77 were added the ligation

buffer at concentration 300-400 uM. The mixture was adjusted to final volumn of 10 mL by addition of 4 mL double distilled water. This mixture was allowed to incubate in a water bath at 37°C for 5 hours. The enzymatic solution was concentrated to 4mL and subjected to ion exchange chromatography (Mono-S). The eluted fractions were collected based on maximal peak height on the chromatogram. Fractions were run on SDS-PAGE gel electrophoresis to verify the presence of di-ubiquitin. This technique was adapted from established literature approach [15].

2.3 Purification of Ub-MESNa for Ub-Prg reaction

A 6 L batch of Ub-MESNa was expressed using pTXB1 vector with ampicillin resistance in *E.coli* BL-21 cells. Ub-MESNa is a fusion construct that consists of ubiquitin, an intein group, and a chitin binding domain. The cells were spun down and resuspended in Ub-MESNa buffer (50mM MES and 300mM NaOAC pH 6). The resuspended mixture was then lysed via French press and cleared via ultra-centrifugation at 100,000 x g. The supernatant was then added to a chitin column that was pre-equilibrated with Ub-MESNa buffer. The column was washed with 400mL Ub-MESNa buffer. An amount of 60mL of elution buffer was added to the column. The elution buffer consists of 120mL Ub-MESNa and 1g of MES. The column was capped to allow overnight incubation of the reaction at 37°C. The reaction was then eluted with remainder of Ub-MESNa buffer and confirmed on SDS-PAGE gel showing an 8.5kDa band.

2.4 Reaction with Propargylamine

An amount of 500uL propargylamine was added to 1.5mL concentrated sample of Ub-MESNa and diluted to 9.5mL with 1M sodium bicarbonate pH 8. This reaction was allowed to incubate overnight at room temperature in the dark. The reaction was dialyzed into Mono-S

buffer (50mM NaOAc, pH 4.5), filtered, and passed through Mono-S column (GE Healthcare). The eluted fractions were collected based on maximal peak height on the chromatogram.

2.5 LotA Primer design and Cloning

Four novel LotA constructs were designed based on secondary prediction model from the online server PSIPRED. LotA full length (FL) was entered in the server to which secondary prediction model was generated. The constructs were designed to cut into the predicted flexible regions of the protein. The primer for construct 1-252 with a cut at Asp252 is XhoI REV 5'-GCATGCCTCGAGTTAATCCAGAAA ACGCTCGCTATCTTC-3. The primer for construct 1-259 with a cut at Lys259 is XhoI REV 5'-GCATGCCTCGAGTTATTTCAAACGTGAGGGTGT CGAATC-3'. The primer for construct 1-269 with a cut at Asp269 is XhoI REV 5'-GCATGCCTCGAGTTAATCACCTCGATAAGCCTCCAAGG- 3'. The last construct 1-285 with a cut at Glu285 is XhoI REV 5'-GCATGCCTCGAGTTACTCTTCAATCAAATCCAA CTGCTCAG-3'. The preceding primers were each mixed with FL template LotA DNA and the corresponding forward primer in pcr premix according to established protocols. The PCR products were verified on gel. Restriction enzyme digest was conducted using BamHI and XhoI followed by ligation.

2.6 UCHL1 R178Q Expression and Purification

The point mutation of WT UCHL1 was generated using Qiagen quik-exchange protocol. The successful point mutation in vector pGEX-6P-1was transformed into *E.coli* BL-21 cells. Cultures were grown to an OD of 0.4-0.6 at 37°C. This was induced with 300 uM IPTG and expressed at 18°C for 16-18 hours. The cells were lysed via French press and cleared via

centrifugation at 100,000 x g for 1 hour. The GST fusion construct was purified using standard GST affinity chromatography techniques. The protein was further purified using size exclusion chromatography S75. The eluted fractions were collected based on maximal peak height on the chromatogram. The same procedure was carried out to purify UCHL1 mutants R178A, E60Q, and E60A.

2.6.1 Primer Design of UCHL1 mutants

The primer for UCHL1 mutant E60A is forward primer (fwd)-CTCACG GCCCAGCATGCAAACTTCAGGAAA and reverse primer (rev)-TTTCCTGAA GTTTGCATGCTGGGCCGTGAG. Mutant E60Q is fwd- CTCACGG CCCAGCATCAAAACTTCAGGAAA and rev- TTTCCTGAAGTTTT GATGCTGGGCCGTGAG. The primer for mutant R178A used fwd- CTCTATGAACTTGAT GGAGCAATGCCTTTTCCGGTG and rev-CACCGGAAAAGG CATTGCTCCATCAAGTTCATAGAG. These point mutations were chosen to investigate the role in rate of activity of two residues R178 and E60 that have strong interactions with the catalytic histidine H161. This is based on crystal structure analysis.

2.7 Protein Crystallization and Structure Determination UCHL1 R178Q

Protein crystallization trials were set up using vapor diffusion method in C4 condition of the Ammonium Sulfate grid screen (0.1M HEPES, 2.4M Ammonium Sulfate, pH 7.4). Small cube shape crystals grew in two days. The crystals were placed in liquid nitrogen for flash cooling with no cryo-protectant. Diffraction data was collected (up to 2.8 Å) at Advanced Photon Source at Argonne National Laboratory and processed using HKL2000 [16]. Data was collected at 100 K on Mar300 CCD detector (Mar USA) at the beamline 23-ID-D. The structure of the

mutant was determined by molecular replacement using UCHL1 R178A H161A as a search model. The molecular replacement solution was obtained in P4212 space group using the program MolRep in CCP4 suite [17].

2.7.1 Novel Protein Crystallization technique for WT UCHL1

The rate of crystallization of WT UCHL1 can be increased significantly by accelerating vapor diffusion. This is done by normal set up of WT UCHL1 (~20mg/mL) in condition 0.1M HEPES, 2.4M Ammonium Sulfate, pH 7.4 on 96 well tray for vapor diffusion. Instead of sealing the tray with tape for normal facilitation of vapor diffusion, leaving the crystallization drop uncovered speeds up the rate of crystallization substantially. The tray can be covered with a lid and the sides of the tray sealed with tape. WT UCHL1 crystals form in as little as two days. WT UCHL1 crystallization done without this set up require over a month. The crystals are well diffracting crystals (~1.8Å). UCHL1 R178Q can also be crystallized using this approach but it is not required as the mutant crystallizes much quicker than the wild type protein.

2.8 Enzymatic Activity Assay for UCHL1 Mutants

Solutions of WT UCHL1 and mutants R178Q, R178A, E60Q, and E60A were diluted to 4nM in reaction buffer (1M Tris pH 7.6, 500mM EDTA, 1% (w/v) BSA, 1mM DTT). The protein was transferred to 96 well tray (25uL). Ub-Rhodamine 110 was added to the well at equivalent volume 25 uL at 360nM to initiate the reaction. The final concentrations in the wells for enzyme and substrate were 2 nM and 180 nM, respectively. The rate of cleavage was monitored at 25°C by TECAN Genios microplate spectrofluorometer at an excitation wavelength of 485nm and emission wavelength of 520nm.

2.9 Circular Dichroism of WT UCHL1 and R178Q

The Circular Dichroism spectra were generated using established protocol by Rashmi *et al*. [18]. Wild type UCHL1 and mutant R178Q were diluted to final concentration of 0.2mg/mL in 100mM sodium phosphate buffer pH 7.4. The CD spectra were recorded on Jasco J-1500 spectrophotometer in the far UV region (200-260nM) in a cuvette with path length of 0.1cm. The ellipticity was monitored at 222nm for thermal melt. The thermal melt was conducted by heating the protein from 20-86°C with temperature gradient of 0.5°C. Data was recorded after every increase of 2°C with four scans at average speed of 100nm/min. The spectrum of the phosphate buffer was used as a blank.

CHAPTER 3. RESULTS AND DISCUSSION: LOTA

3.1 Investigations into LotA First Catalytic Domain

Full length LotA is 744 residues long and contains three domains. A representative domain diagram is depicted in Figure 3.1. Kubori *et al.* have shown that a construct spanning 1-290 residues of LotA cleaves K6 di-ubiquitin [4], which is the first catalytic domain of the effector. LotA shares most structural similarity with the human DUB OTU6b [4]. Komander *et al.* have shown that DUBs from the OTU family possess strict specificity restraints [9]. In order to gain insight into the K6 linkage specificity further biochemical analysis of the first catalytic domain from construct 1-290 was necessary.

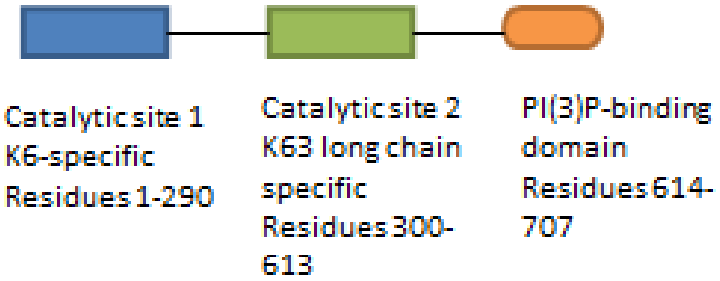

Figure 3.1. Domain diagram of LotA.

Figure 3.1 shows the probable domain arrangement for LotA. The first catalytic domain specific for K6 di-ubiquitin consist of residues 1-290 as confirmed by Kubori *et al* [4]. The second catalytic domain specific for long chains of K63 linked ubiquitin consists of residues 300-613 [4]. The final domain is a lipid PI(3)P-binding domain consisting of residues 614-707 [4].

3.1.1 Expression and Purification $LotA_{1\text{-}290}$

In this work, the biochemical findings of Kubori *et al.* were verified and further explored through Michaelis-Menten kinetics analysis of the 1-290 construct for LotA. Expression and purification of $LotA_{1\text{-}290}$ was successfully achieved yielding approximately 37mg/mL of protein when concentrated to 2mL. Figure 3.2 shows the purification gel. The GST subtraction product is pure showing successful removal of GST tag.

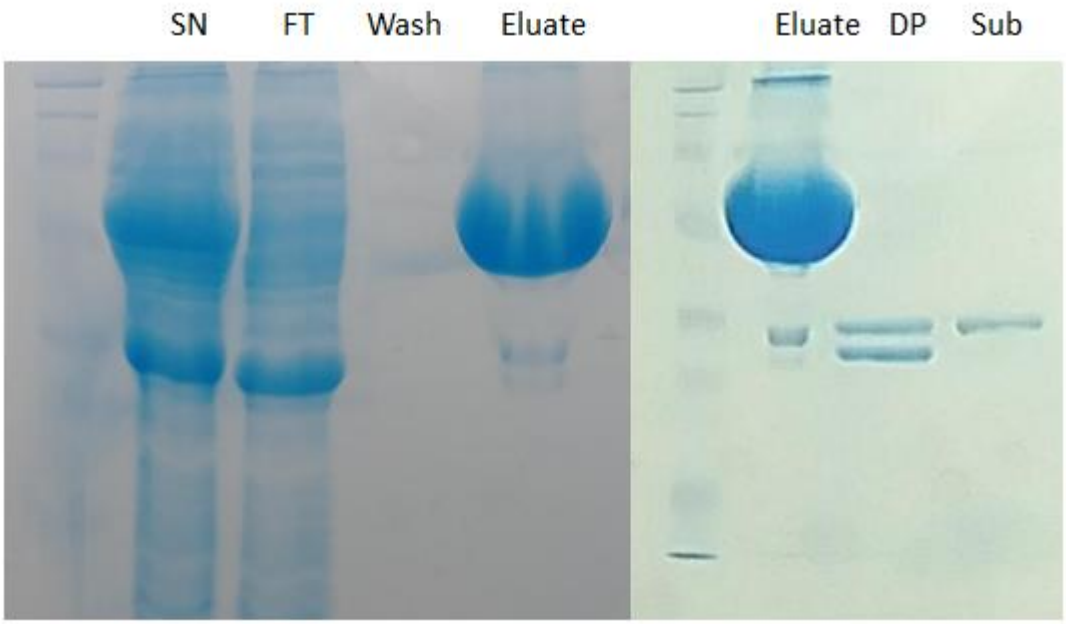

Figure 3.2. Purification gel of $LotA_{1\text{-}290}$.

The subtraction product was concentrated to 4mL and subjected to size exclusion chromatography (SEC). The protein eluted at volume 52mL with eluted fractions being 2mL. Figure 3.3 shows the chromatogram for the size exclusion of $LotA_{1\text{-}290.}$ Upon the successful expression and purification of $LotA_{1\text{-}290}$ the protein was used for biochemical assays.

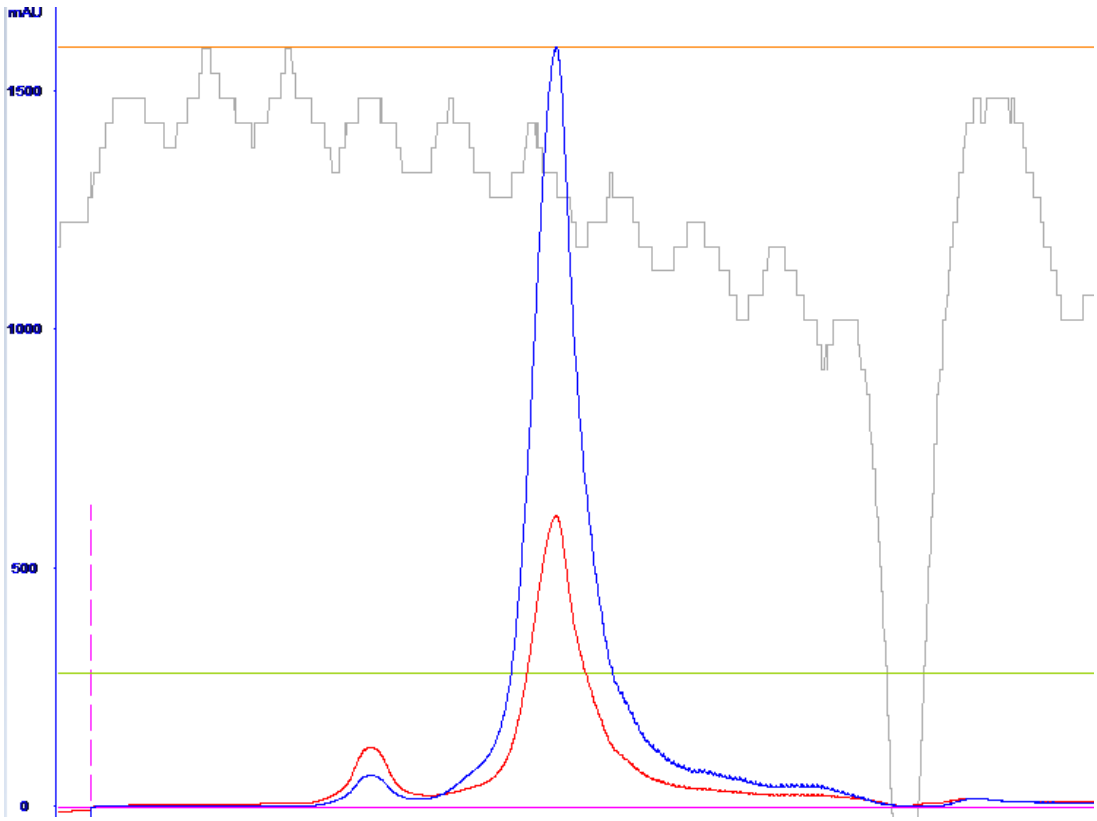

Figure 3.3 SEC Chromatogram of $LotA_{1-290}$.

3.1.2 Preparation of K6-Ub_2

The first biochemical assay employed was to determine linkage specificity of $LotA_{1-290}$. This was verification of the work of Kubori *et al* [4]. The substrate K6-Ub_2 was enzymatically prepared using the bacterial E3 enzyme NleL as described in the experimental methods. The chromatogram (Mono S) of the reaction product is shown in Figure 3.4. Successful separation of di-ubiquitin from the unreacted monoubiquitin was achieved with ion exchange Mono S as shown by the three peaks in figure 3.4. The di-ubiquitin eluted at volume 36mL with elution fraction of 1.5mL. This was confirmed by SDS-PAGE a seen in Figure 3.5. The concentration of the K6-Ub_2 was 300 uM when concentrated to 200 uL.

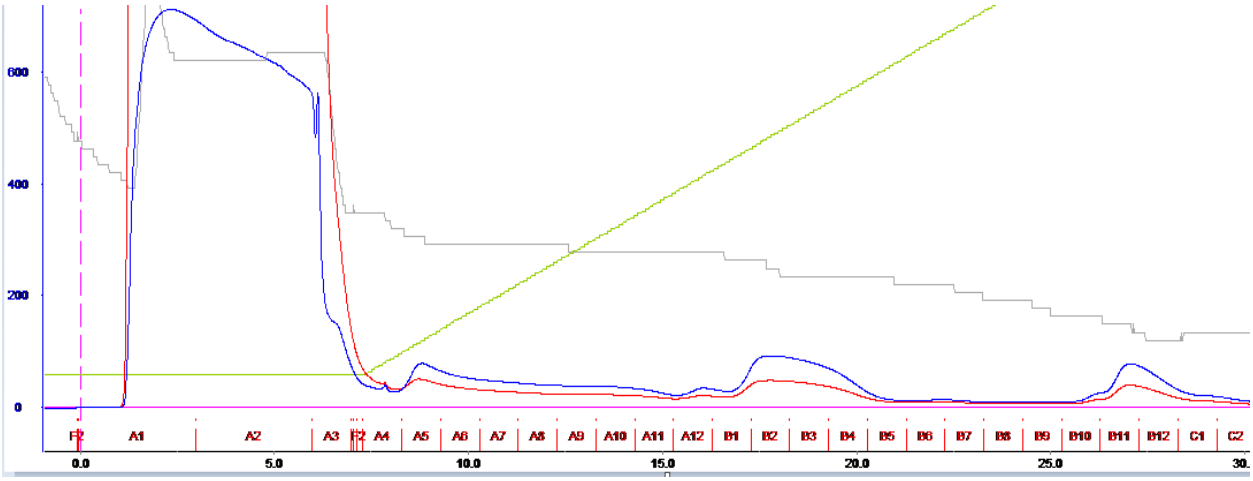

Figure 3.4 Ion exchange Mono S chromatogram for K6-Ub_2 reaction product.

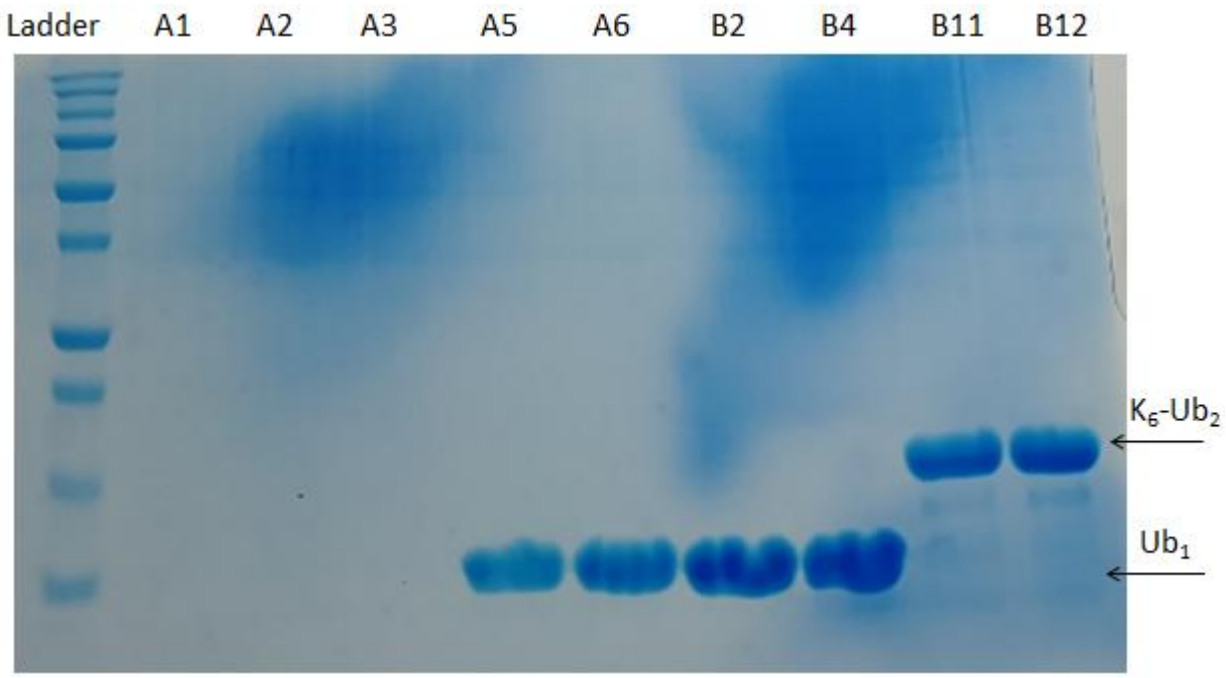

Figure 3.5 SDS PAGE gel of Mono S fraction for K6-Ub_2 reaction.

3.1.3 Specificity Assay for $LotA_{1-290}$

The purified K6-Ub_2 was used in specificity assay for $LotA_{1-290}$. This assay was done in similar manner to Kubori *et al*. differing in concentration amounts used and SDS PAGE gel

electrophoresis. $LotA_{1-290}$ is clearly specific for K6-Ub_2 as seen in Figure 3.6. The other chain types tested were resistant to hydrolysis by LotA. The reaction condition for the specificity assay was 1 uM enzyme and 30 uM substrate at time 0 and 1 hour. Full cleavage of K6-Ub_2 by $LotA_{1-290}$ was observed in the one hour time frame at the reported concentrations. To conduct Michaelis-Menten kinetics experiments the reaction system would need to be at initial velocity. A time dependent assay was done to establish initial velocity shown in the right panel of Figure 3.6. The enzyme concentration was lowered to 25nM for the time dependence assay.

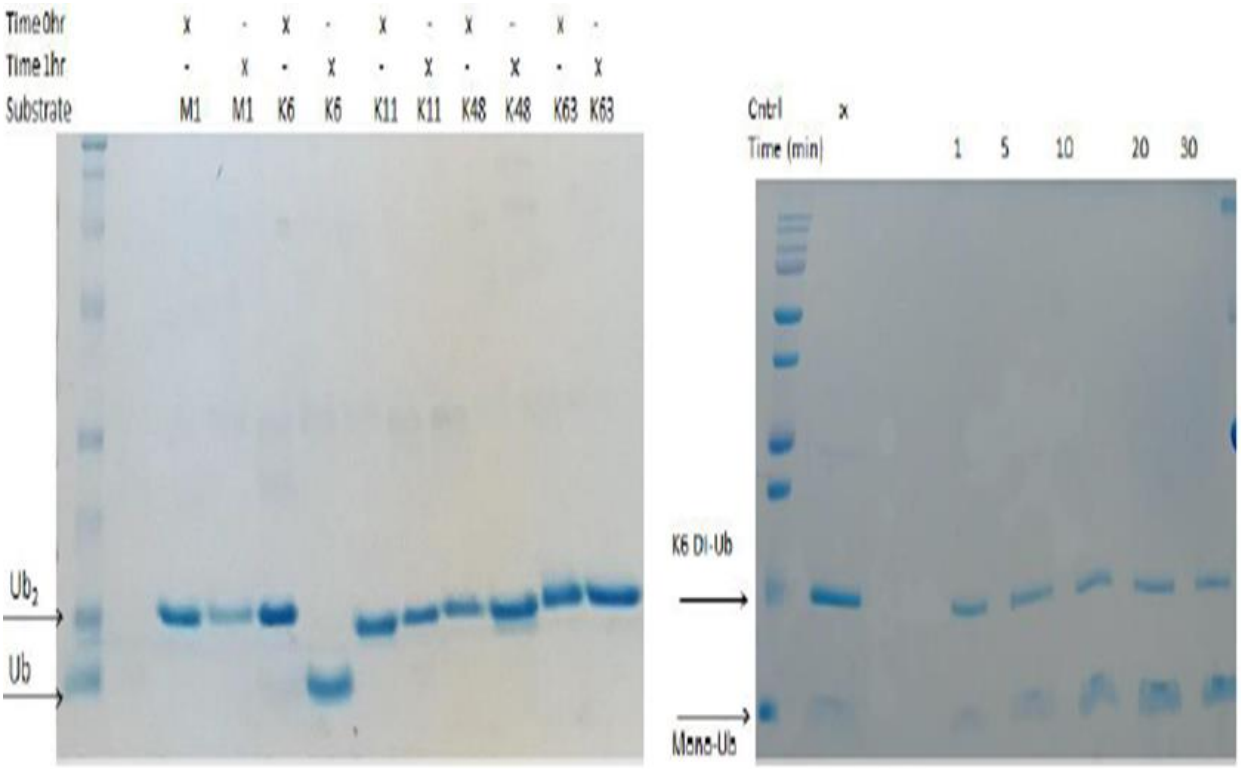

Figure 3.6 Specificity assay for $LotA_{1-290}$ (left) and time dependent assay (right).

3.1.4 $LotA_{1-290}$ Kinetic Profile

$LotA_{1-290}$ has not been kinetically profiled until this work. Using the information from the time dependent assay shown in Figure 3.6, Michaelis-Menten kinetics experiments were

conducted. The reaction time was 15 minutes with enzyme concentration of 25 nM. The substrate concentrations used were 10, 20, 40, and 80 uM. The plot of the data points can be seen in Figure 3.7. The fitting of the data points is shown in Figure 3.8 using an online server. The equation of the fit is y= (0.1044x)/(12.89+x). The Vmax is 0.1044 uM/s and the k_m is 12.89 uM. The k_{cat} is 4.176 s^{-1}. The k_{cat}/k_m (catalytic efficiency) is 0.324. The kinetic parameters are shown in Table 3.1. When compared to SdeA, the most characterized *Legionella* DUB, $LotA_{1-290}$ has approximately four fold higher k_{cat} and 10 fold lower k_m for their respective substrates [5]. LotA thus can be considered a more efficient enzyme for K6-Ub_2 hydrolysis than SdeA is for K63 hydrolysis.

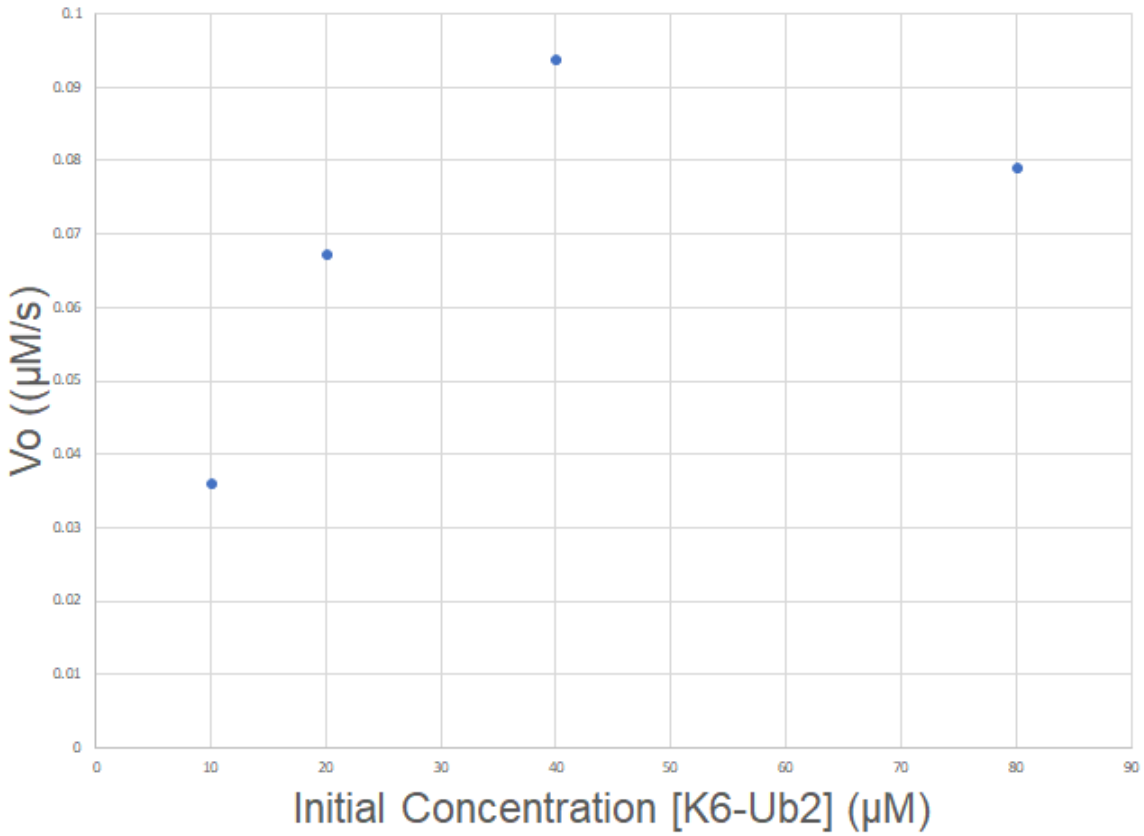

Figure 3.7 Plot of $LotA_{1-290}$ kinetic experiment.

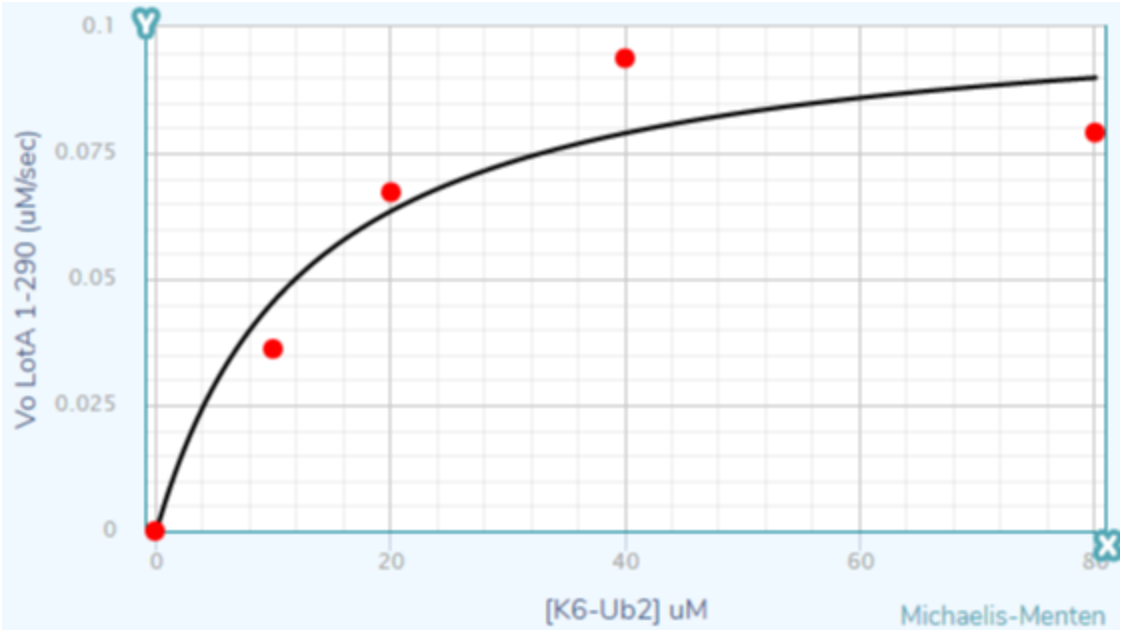

Figure 3.8 Fitting of Michaelis-Menten data.

Table 3.1Kinetic Parameters $LotA_{1-290}$

k_{cat}	k_m	K_{cat}/k_m
4.176 s^{-1}	12.89 uM	0.324 uM/s

3.1.5 Activity Probe Shift Assay

The reactivity of $LotA_{1-290}$ with Ub-parpargylamine (Ub-Pa) was verified and compared with Ub-VME. $LotA_{1-290}$ has clear preference for Ub-Pa as seen in Figure 3.9 left panel compared to right panel. The shift titrations were conducted according to established protocol [16]. There is more formation of covalent adduct with Ub-Pa than with Ub-VME. This trend has been observed with various human OTU DUBS [9]. The OTU like structure of $LotA_{1-290}$ shows strict restraints as seen by singular preference in specificity for substrate and selectivity for activity based probes.

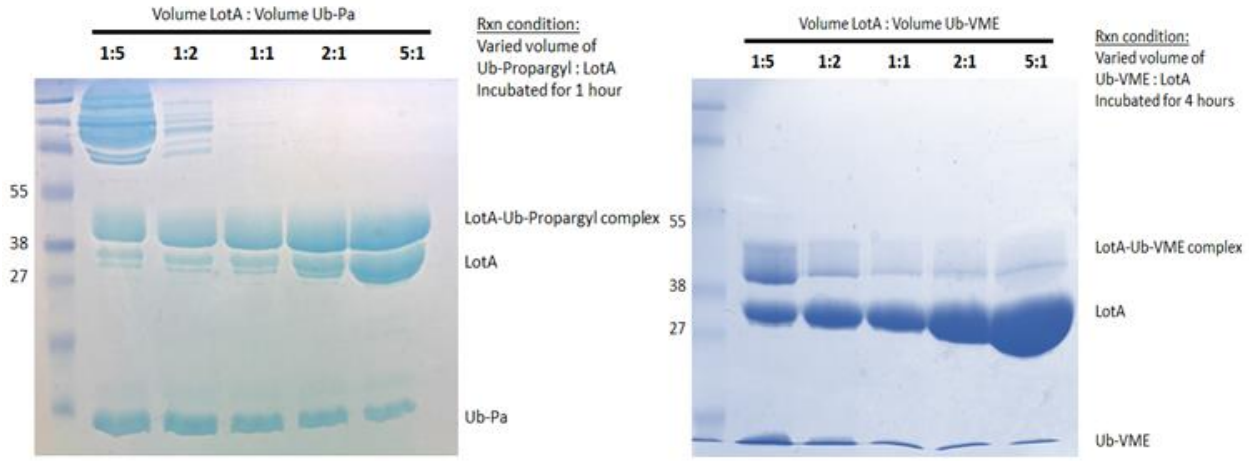

Figure 3.9 Comparison of Activity based probe shift assay; Ub-Pa (left), Ub-VME (right).

3.2 Further Insight into LotA; Identification of Distal Site Interacting Residues of Domain 1

Four novel constructs of LotA were designed to elucidate structural and biochemical information of the first catalytic domain. The four truncations designed for LotA are: 1-252, 1-259, 1-269, and 1-285. An interesting finding was that all the constructs completely cleave K6-Ub_2 when using sufficiently high amounts (4 uM enzyme; 35 uM substrate). This result is indistinguishable from the 1-290 construct. Figure 3.10 shows even the smallest construct (1-252) is capable of cleaving K6-Ub_2 at the noted concentrations. The distinction is drawn with the Ub-Pa shift assay. The larger constructs (1-269; 1-285) are modified by the activity probe to the same level as the $LotA_{1\text{-}290}$. Figure 3.11 shows the Ub-Pa shift assay with constructs 1-269. The smaller constructs 1-252 and 1-259 show decreased reactivity towards Ub-Pa. Figure 3.12 shows the activity probe shift assay of 1-252 and 1-259. The activity based probe Ub-Pa mimics the distal binding site of ubiquitin chain. The reduced affinity of the smaller constructs for Ub-Pa suggests a loss in distal site binding/interacting residues. Residues 259-269 are likely involved in

distal site recognition or binding of di-ubiquitin chains. The loss of these residues contributes to decreased modification by Ub-Pa. One can predict a notable difference in km value when comparing the kinetic profile of $LotA_{1-259}$ versus $LotA_{1-269}$.

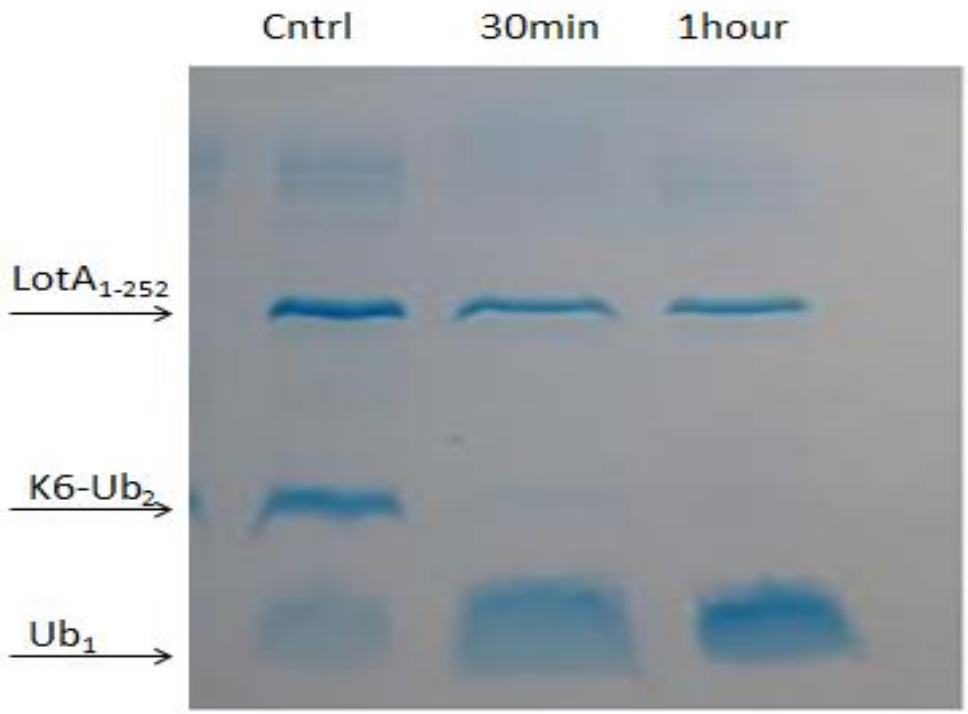

Figure 3.10 $LotA_{1-252}$ cleavage assay at E:S concentrations 4 uM and 35 uM respectively.

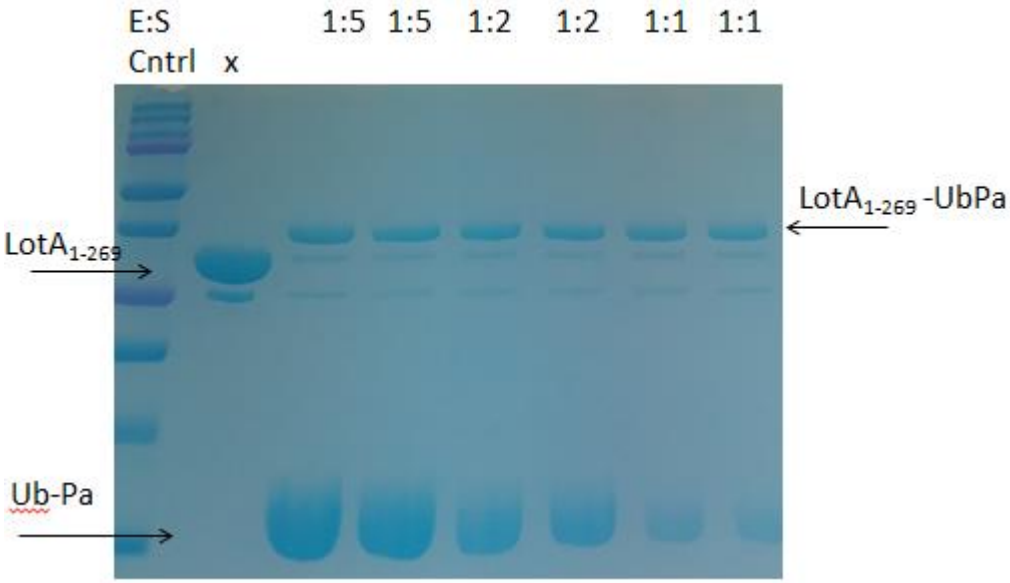

Figure 3.11 $LotA_{1-269}$ Ub-Pa shift assay.

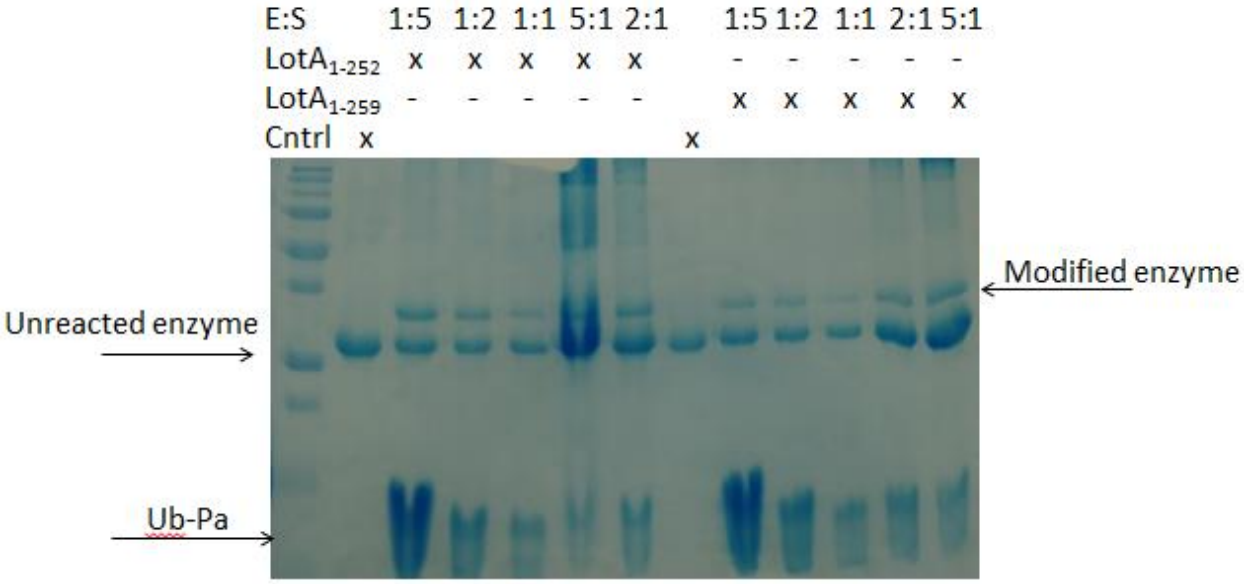

Figure 3.12 $LotA_{1-252}$ and $LotA_{1-259}$ activity shift assay.

3.3 Expression and Activity of LotA Second Catalytic Domain

My colleague Kedar in the Das lab generated a construct for the second catalytic domain of LotA (293-613). I successfully expressed and purified the protein $LotA_{293-613}$ (5mg/mL). The purification gel is shown in Figure 3.13. I conducted an activity based probe shift assay to examine if the construct can be modified by Ub-Pa. The result is shown in Figure 3.14. $LotA_{293-613}$ cannot be modified by Ub-Pa. This is opposite of the first catalytic domain $LotA_{1-290}$ which readily reacts with Ub-Pa.

A preliminary in trans assay was conducted to examine if $LotA_{293-613}$ required help of the first domain to react with Ub-Pa. The Ub-Pa assay was done with $LotA_{293-613}$ in presence of catalytically inactive construct of the first domain ($LotA_{1-270}$). Both proteins were at same concentration. There appeared to be some modification (data not shown) suggesting that LotA second domain likely cooperates with the first domain for activity and/or recognition.

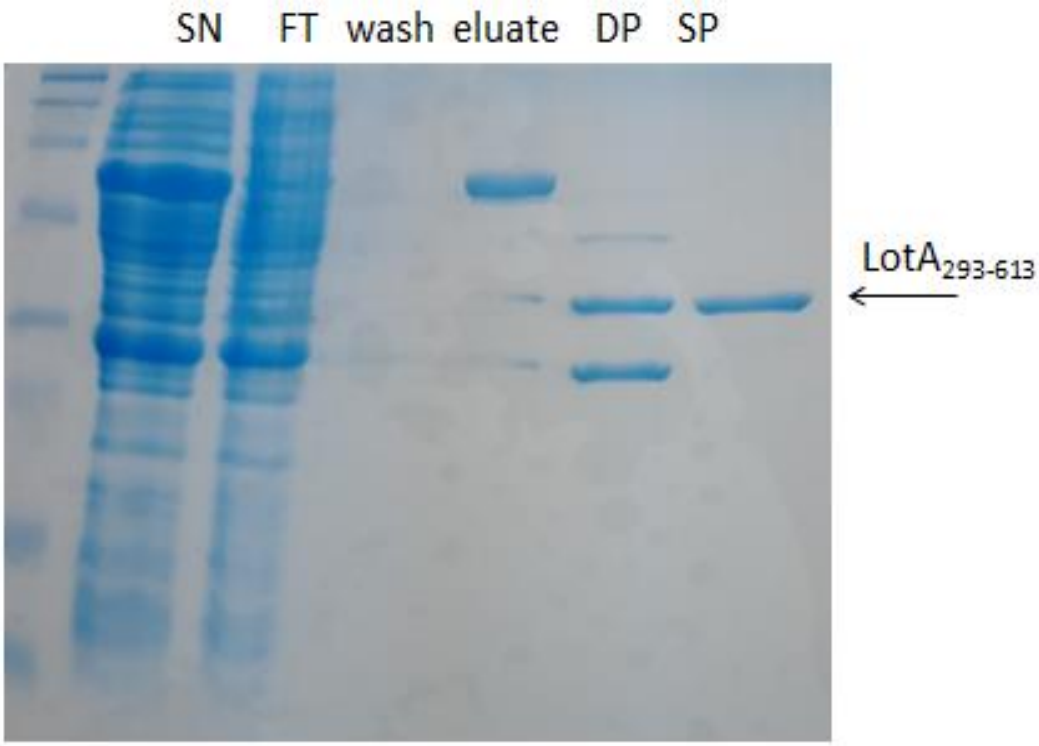

Figure 3.13 SDS PAGE gel of $LotA_{293-613}$ Purification.

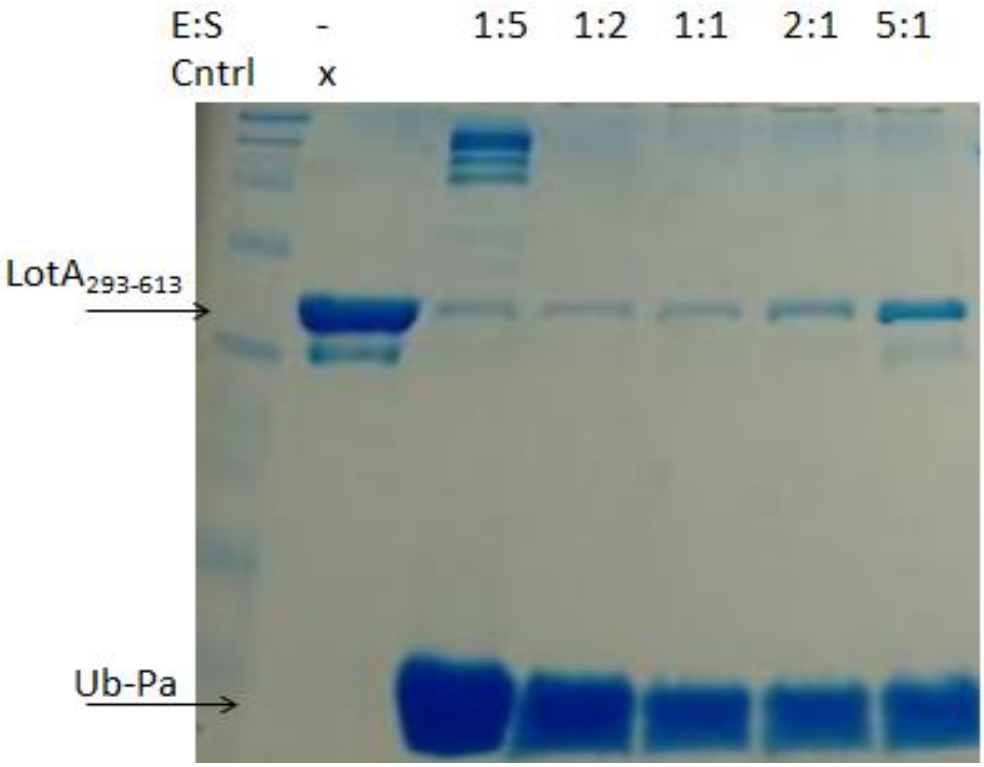

Figure 3.14 The Ub-Pa shift assay with $LotA_{293-613}$. This construct is unreactive on its own.

CHAPTER 4. RESULTS AND DISCUSSION UCHL1 R178Q

4.1 Structural Insight into UCHL1 R178Q

The UCHL1 mutant R178Q was reported to have significantly enhanced catalytic activity compared to the WT UCHL1 [14]. This mutant is suggested to provide protection against early onset progressive neurodegeneration with optical atrophy [14]. The question remaining was how the glutamine point mutation contributes to higher activity? Structural insight seemed the most logical approach to answer this question.

To begin, the protein was successfully expressed and purified following protocol stated in the experimental methods section. SDS-PAGE analysis of the purification samples is shown in Figure 4.1-4.3. The chromatogram showed splitting of peak with maximal heights at elution volume 74 and 82 mL can be seen in Figure 4.2. The protein for peak at elution volume 82 mL was used for structural and biochemical studies. This batch of protein crystallized and showed enhanced activity comparable to literature. The S75 fractions corresponding to peak height elution volume 82mL were pooled and concentrated to 1.5mL with concentration 35mg/mL based on nanodrop estimate absorbance at 280nm.

The mutant was immediately subjected to crystallization trials starting with C4 condition (0.1M HEPES, 2.4 Ammonium Sulfate, pH7.4) of the A/S grid screen. This condition was chosen as the WT had been successfully crystallized in this condition. The mutant crystallized in the C4 condition very quickly (within 2 days). This is considerably faster than normal WT crystallization in the same condition which takes a month. The crystals appeared as small cubes and diffracted to 2.8 Å resolution. Figure 4.4 shows an image of the crystals. Although the crystals grow fast there is sacrifice to diffraction quality when compared to WT.

Figure 4.1 Purification gel of UCHL1 R178Q.

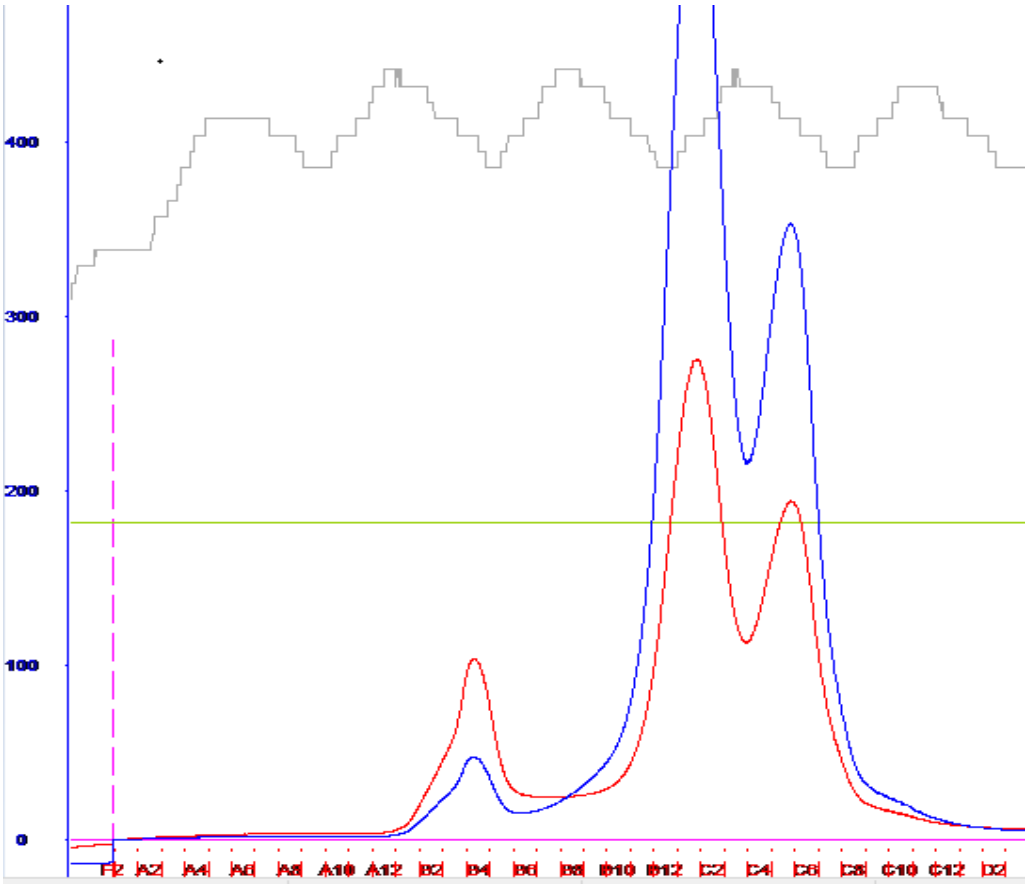

Figure 4.2 Chromatogram of S75 SEC purification of UCHL1 R178Q.

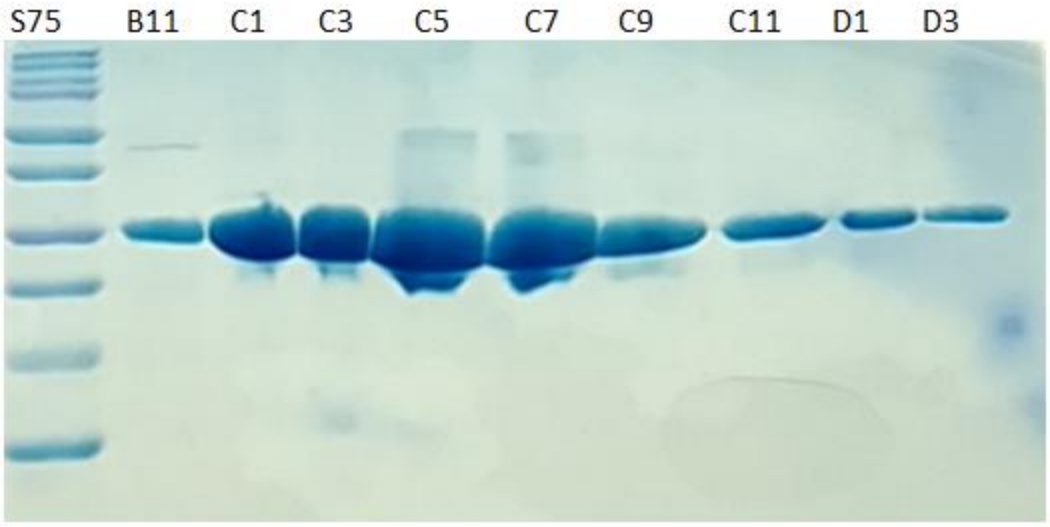

Figure 4.3 SDS-PAGE gel of SEC fractions for UCHL1 R178Q. Fractions C5 and onward were used for further studies.

Figure 4.4 UCHL1 R178Q crystals from C4 condition.

The search model used for Molrep was UCHL1 R178A and H161A. This was done to reduce bias. The model had clear density for UCHL1 Q178 and H161, where the respective

sidechains can easily be built in. This is shown in Figure 4.5. Upon inspection of the crystal structure R178Q appears to share the same conformation as in the WT. It was believed that glutamine mutant destabilizes the position of the catalytic histidine (H161) allowing for closer positioning to the catalytic cysteine (C90). The closer arrangement would be linked to the enhanced activity. This was not observed in the crystal structure of R178Q. The catalytic histidine H161 is 7 Ǻ away from C90. This is shown in Figure 4.6. This is closer than the WT arrangement where H161 is 8.7Ǻ away from C90 [12]. The low resolution data for R178Q calls into question how accurate are the interatomic distances. With this in hand, the change in position of H161 from WT to R178Q could be negligible.

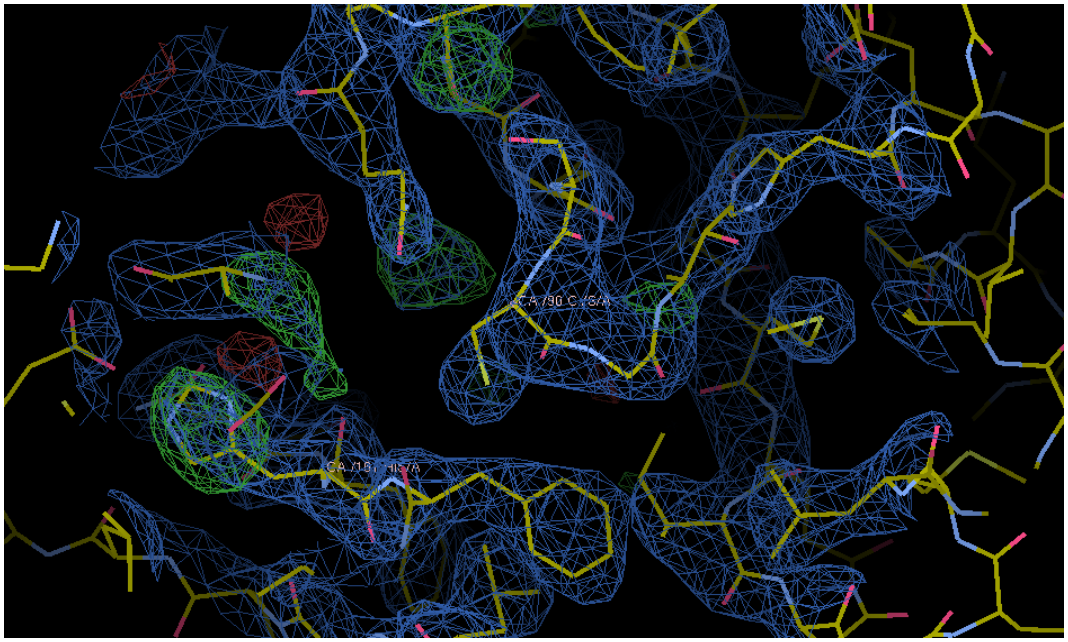

Figure 4.5 Electron density map UCHL1 R178Q. Density is shown for H161 and Q178.

It was observed in the crystal structure of R178Q that residue E60 maintains a strong interaction with H161 with distance of 2.1 Ǻ. This is shown in Figure 4.7. Residue E60 also maintains similar strong interaction with H161 in WT UCHL1. This then begs the question as to

what role residues R178 and E60 have on the rate of activity of UCHL1. Biochemical analysis would help shed light onto their roles.

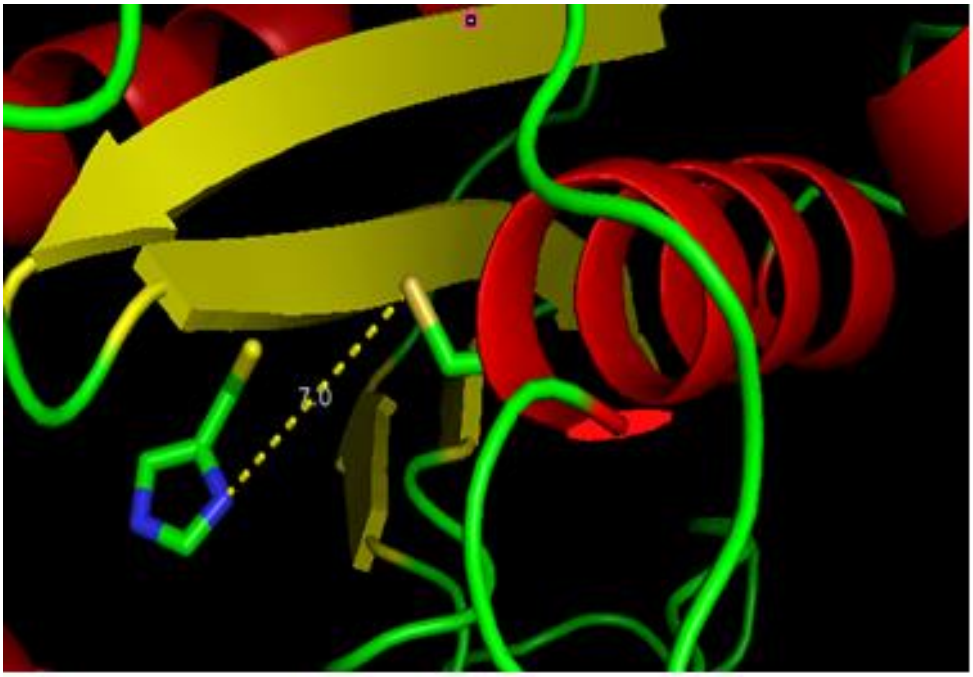

Figure 4.6 The distance of H161 and C90 for the UCHL1 R178Q structure.

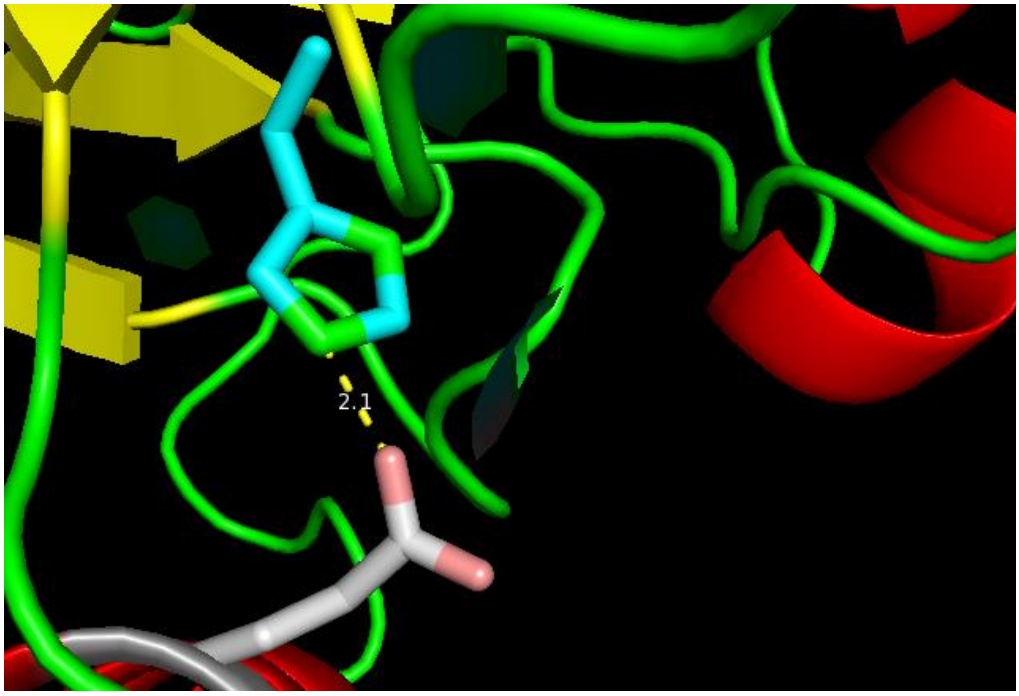

Figure 4.7 Residue E60 forming close interaction with H161 of R178Q crystal structure.

4.2 Biochemical Analysis

The tight interactions of residues R178 and E60 provides opportunity to examine the effect these residues have on activity on UCHL1. For the R178Q mutant, does the glutamine mutant have any importance or does the loss of interaction dictate the enhanced activity? Since residue E60 has strong interaction with H161, can a mutation to glutamine at that position yield similar result as R178Q? These are the questions we sought to answer.

The mutants UCHL1 R178A, E60Q, and E60A were generated. These mutants were tested against UCHL1 R178Q and WT in Ub-Rhodamine assay. The results are shown in Figure 4.8. It appears that the glutamine mutant at position 178 imparts both a residue type and positional impact on the rate of the activity of UCHL1. This is seen when comparing R178Q with R178A. Both mutants correspond to enhanced activity when compared to WT but R178Q is

higher. This means that the residue type at 178 is important for increased activity of the enzyme. The mutants E60Q/A show decreased activity when compared to WT indicating that the tight interaction of residue E60 is needed to maintain basal activity.

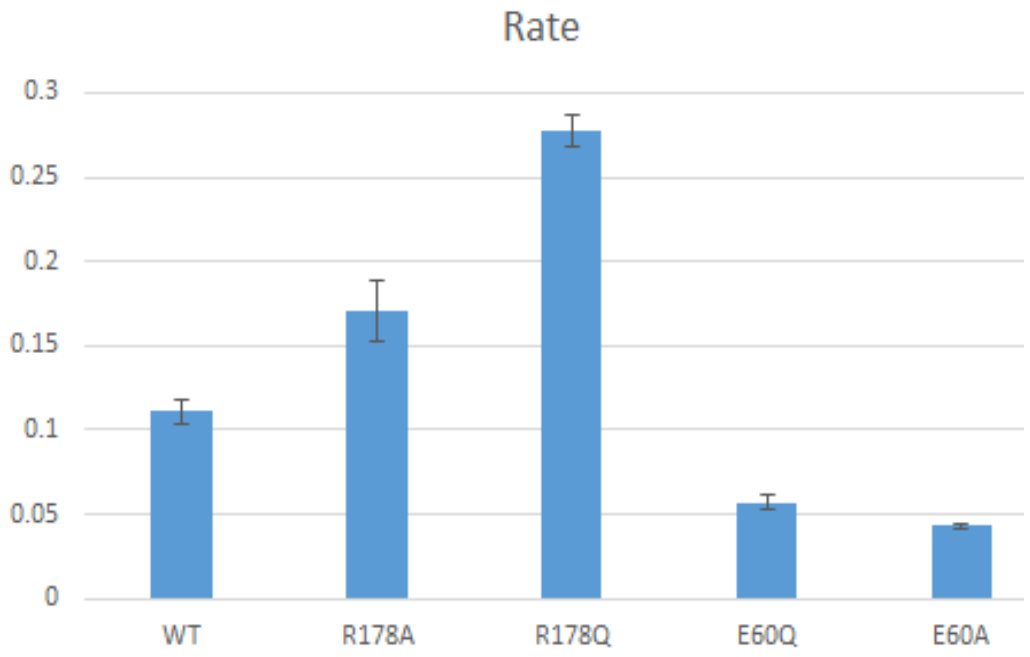

Figure 4.8 Ub-Rho activity assay on UCHL1 WT and mutants.

4.2.1 Kinetic Profile WT UCHL1 vs R178Q

My colleague Aaron of the Flaherty lab collected Michaelis-Menten data for WT UCHL1 compared to R178Q. The data is shown in Figure 4.9 and Table 4.1. It appears R178Q undergoes a nearly 5-fold increase in k_{cat} and approximately 6-fold increase in k_m when compared to WT. A binding analysis to ubiquitin is needed to understand the increase in k_m. It could be that R178Q dimerizes more readily in solution than WT. This may have a negative impact on binding to substrate. An AUC experiment could be done to test this theory.

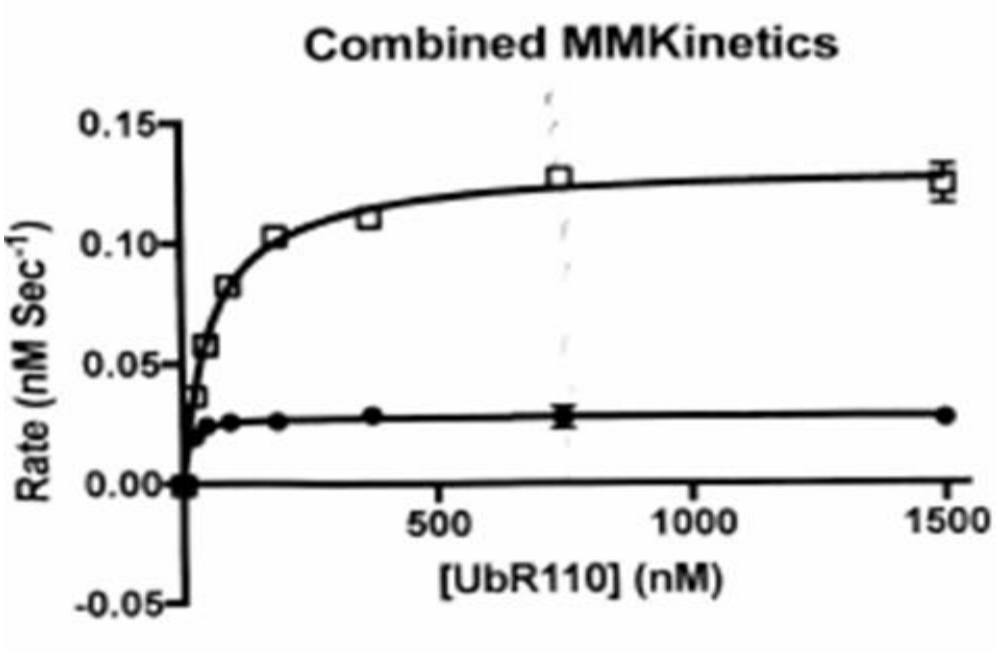

Figure 4.9 Kinetic profiles of UCHL1 WT and R178Q.

Table 4.1 Kinetic ParametersUCHL1 WT and R178Q

Enzyme	k_{cat}	k_m
UCHL1 WT	0.02807 s^{-1}	9.383 nM
UCHL1 R178Q	0.1316 s^{-1}	57.87 nM

4.3 Stability Analysis

A CD thermal melting experiment was done to determine if the UCHL1 R178Q mutant was less stable than WT. The loss in stability could be correlated to the enhanced activity. The result is shown in Figure 4.10. There is very little difference in melting temperature (Tm) of the two proteins. The R178Q mutant has Tm of about 52°C and WT is approximately 55°C. It appears that R178Q is only slightly less stable than WT.

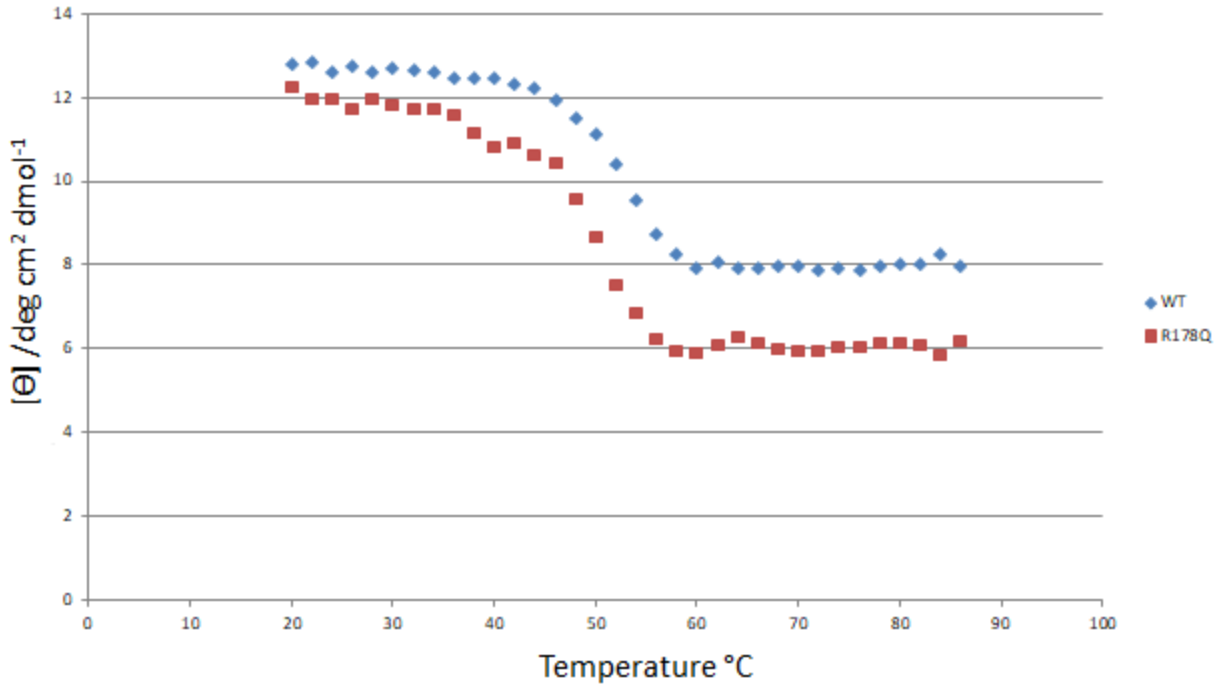

Figure 4.10 CD thermal melt of UCHL1 WT and R178Q.

4.4 Further Discussions

The crystal structure of UCHL1 R178Q does not provide definitive insight into why the mutant is more active than WT. The catalytic histidine is still misaligned being 7 Å away from C90. The biochemical data suggest that both the residue and position 178 are important for the enhanced catalytic activity. The stability profile of mutant R178Q and WT are similar, suggesting that the enhanced activity may not be exclusively linked to loss of stability.

The mutant crystallizes as a dimer, as does WT. This is shown in Figure 4.11. When comparing the SEC (S75) chromatograms of WT and mutant R178Q it is noted there is a splitting of major peak for both proteins. The splitting is opposite in orientation for the two proteins. This is shown in Figure 4.12. For WT, the larger of the split peaks is at the greater elution volume whilst for the mutant R178Q, the larger of the split peaks is at the lesser elution

volumes. This could be an indication of dimerization of the mutant R178Q. An analytical ultracentrifugation (AUC) experiment can be done to verify this. If indeed the UCHL1 R178Q mutant does undergo significant dimerization this could be correlated to the enhanced activity. Such example was shown by Komander *et al*. in recent paper on USP25 and USP28 [20]. The oligomerization state of USP25 and USP28 determines the DUB activity of the two enzymes [20].

UCHL1 activity still has unanswered questions. Bishop *et al*. reported UCHL1 can cleave polyubiquitin when co-transfected with a plasmid containing a polyubiquitin gene [21]. This evidence opposes the dominant view that UCHL1 only cleaves ubiquitin from unstructured substrates [22]. With new findings about UCHL1 activity, one should be open to examining the possible dimerization effect on activity of mutant R178Q. The possible dimerization of R178Q could very well explain the drastic rate increase in crystallization of R178Q compared to WT. R178Q can crystallize in two days while WT can take over a month under the exact same condition.

I have developed a technique that drastically increases the rate of crystallization for WT UCHL1. This is done by letting the crystallization drop dry out under a closed system for about 2-3 days. The crystals appear in that time. The drying drop likely condenses molecules facilitating dimerization in transition to solid state. If dimerization is required for UCHL1 crystallization, then this would explain why the mutant R178Q crystalizes so readily.

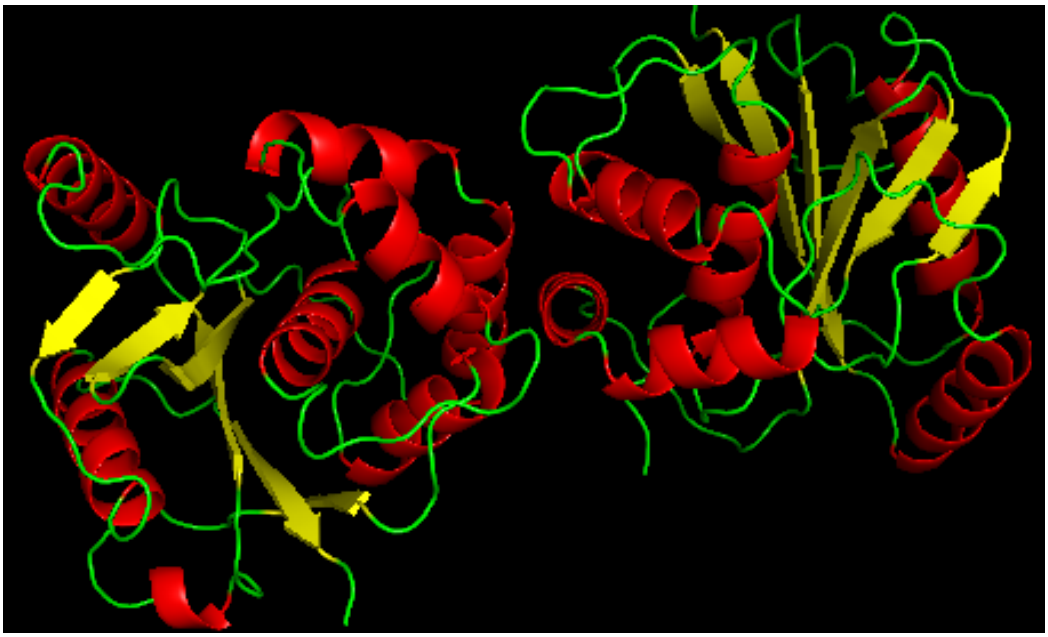

Figure 4.11 UCHL1 R178Q existing as dimer in crystal structure.

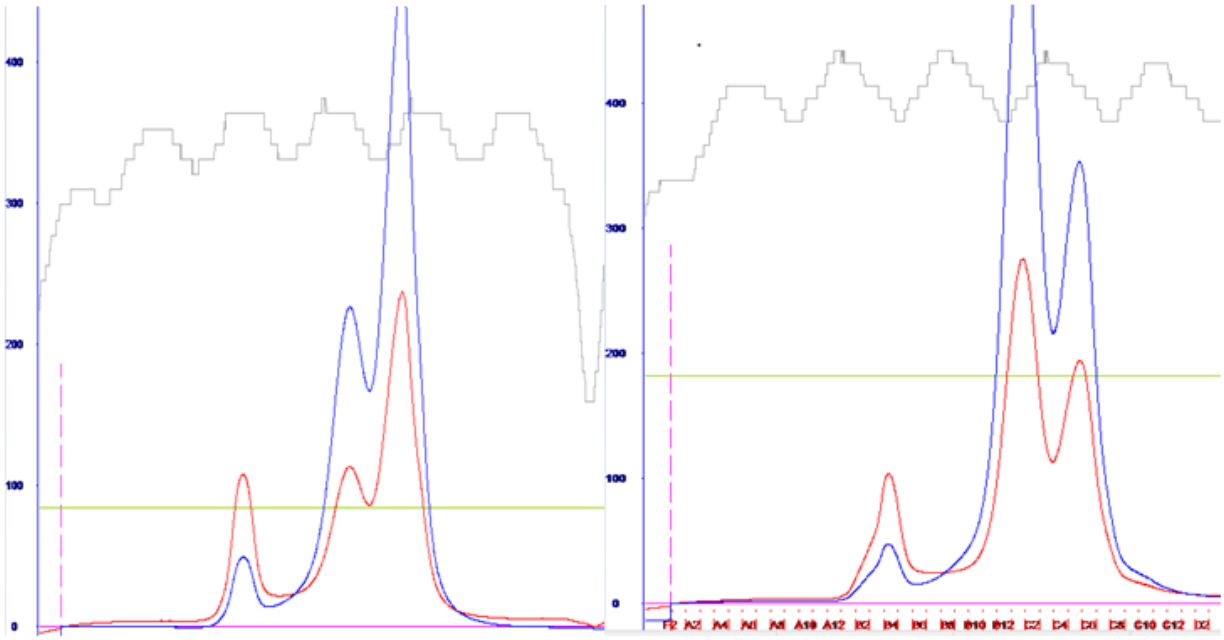

Figure 4.12 Comparison of SEC (S75) chromatograms for WT (left) and mutant R178Q (right). The splitting of the major peak is opposite for the two proteins.

CHAPTER 5. CONCLUSION

5.1 LotA

The *Legionella pneumophila* bacterial effector LotA is needed for organism survival upon infection [4]. LotA possess two catalytic domains with different preference and level of activity [4]. This work aimed at understanding the biochemical function of the first catalytic domain. The specificity requirement shown by Kubori *et al*. of $LotA_{1-290}$ was confirmed in this study [4]. Michaelis-Menten kinetics characterization was done on $LotA_{1-290}$, revealing it to be a more efficient enzyme than SdeA. The truncations of LotA (1-259, 1-269) reveal important residues involved in interactions with the distal binding site of ubiquitin chain. This is based on the significant difference in activity with activity based probe Ub-Pa. This information would be useful for structural studies of LotA. The two published crystal structures of DUBs from *Legionella* were crystallized with constructs of 1-200 [5,8]. Such truncations would likely be difficult to generate a complex of LotA in structural studies when losing residues below 269.

The second catalytic domain on its own was unreactive to Ub-Pa, highlighting the contrast in substrate preference of the two domains. Preliminary data suggests that reactivity to Ub-Pa is slightly enhanced for $LotA_{293-613}$ in the presence of an inactive first domain construct.

The role of K6 linked ubiquitin chain in the cell is still unclear [23]. K63 linked ubiquitin is more characterized [23]. This highlights the need for structural studies on both the domains of LotA.

5.2 UCHL1 R178Q

The UCHL1 mutant R178Q is significantly more active than its WT counterpart. UCHL1 R178Q protects against early onset progressive neurodegeneration with optical atrophy [14]. The aim of this work was to discern how the mutant achieved enhanced activity. A structural approach was a logical first step. The mutant R178Q was crystallized and a data set was collected. The structure is currently undergoing further refinement but enough information was obtained by latest models for analysis.

The catalytic H161 is still in a misaligned position with respect to catalytic C90. The biochemical activity assay showed that the residue and the 178 position are important for enhancing the activity of R178Q. Michaelis-Menten kinetic data show sizeable increase to both k_{cat} and k_m for R178Q in respect to WT. The CD thermal melt only showed slight change in melting temperature for R178Q from WT. Further clues to the reason for enhanced activity of UCHL1 R178Q can be inferred from the SEC (S75) chromatogram profile. There may be dimerization population for R178Q. This would need to be confirmed by sedimentation studies. If indeed R178Q dimerizes, that could potentially be reason for the enhanced activity.

REFERENCES

1. Komander D, Rape M (2012) The ubiquitin code. *Annu. Rev. Biochem.* 81:203–29.

2. Lv Z, Williams KM, Yuan L, Atkison JH, & Olsen SK (2018) Crystal structure of a human ubiquitin E1-ubiquitin complex reveals conserved functional elements essential for activity. *J.Biol.Chem*. 293:18337-18352.

3. Kwasna D, *et al.* (2018) Discovery and Characterization of ZUFSP/ZUP1, a Distinct Deubiquitinase Class Important for Genome Stability. *Mol Cell*. 70(1):150-164.

4. Kubori T, Kitao T, Ando H, Nagai H (2018) LotA, a Legionella deubiquitinase, has dual catalytic activity and contributes to intracellular growth. *Cell Microbiol*.e12840.

5. Sheedlo MJ, *et al. (2015)* Structural basis of substrate recognition by a bacterial deubiquitinase important for dynamics of phagosome ubiquitination. *PNAS*. 112 (49) 15090-15095.

6. Qiu J, *et al.* (2016) Ubiquitination independent of E1 and E2 enzymes by bacterial effectors. *Nature*. 533(7601): 120–124.

7. Urbanus ML, *et al*. (2016) Diverse mechanisms of metaeffector activity in an intracellular bacterial pathogen, Legionella pneumophila. *Mol Syst Biol*.12:893.

8. Wan M, Wang X, *et al*. (2019) A bacterial effector deubiquitinase specifically hydrolyses linear ubiquitin chains to inhibit host inflammatory signalling. *Nat Microbiol*. (8):1282-1293.

9. Mevissen T.E.T,*et al.* (2013) OTU Deubiquitinases Reveal Mechanisms of Linkage Specificity and Enable Ubiquitin Chain Restriction Analysis. *Cell*. 154 (1): 169-184.

10. Leroy E, *et al.* (1998) The ubiquitin pathway in Parkinson's disease. *Nature*. 395: 451-452.

11. Jin Y, *et al.* (2017) Prognostic potential and oncogenic effects of UCH-L1 expression in hilar cholangiocarcinoma. *Int J Clin Exp Pathol*. 10(11):10802-10811.

12. Das C, *et al.* (2006) Structural basis for conformational plasticity of the Parkinson's disease-associated ubiquitin hydrolase UCH-L1. *PNAS*. 103: 4675-4680.

13. Boudreaux DA, *et al*. (2010) Ubiquitin vinyl methyl ester binding orients the misaligned active site of the ubiquitin hydrolase UCHL1 into productive conformation. *PNAS*. 107: 9117-9122.

14. Rydning SL, *et al.* (2017) Novel *UCHL1* mutations reveal new insights into ubiquitin processing. *Hum Mol Gen*. 26 (6): 1031-1040.

15. Hospenthal MK, Freund S.M.V, & Komander D (2013) Assembly, analysis and architecture of atypical ubiquitin chains. *NSMB*. 20(5):555-565.

16. Otwinowski Z, Minor W (1997) Processing of X-ray diffraction data collected in oscillation mode. *Methods Enzymol*. 276(partA): 307-326.

17. Murshudov G.N, Vagin A.A, Dodson E.J (1997) Refinement of Macromolecular Structures by the Maximum-Likelihood Method. *Acta Crystallogr D*. 53: 240-255.

18. Bueno AN, Shrestha RK, *et al*. (2015) Dynamics of an active-site flap contributes to catalysis in a JAMM family metallo deubiquitinase. *Biochem*. 54: 6038−6051.

19. Borodovsky A, *et al.* (2001) A novel active site-directed probe specific for deubiquitylating enzymes reveals proteasome association of USP14. *EMBO J*. 20(18): 5187-5196.

20. Gersch M, *et al.* (2019) Distinct USP25 and USP28 Oligomerization States Regulate Deubiquitinating Activity. *Mol Cell*. 74(3): 436-451.

21. Bishop P, Rocca D, & Henley J (2016) Ubiquitin C-terminal hydrolase L1 (UCH-L1): structure, distribution and roles in brain function and dysfunction. *Biochem J.* 473(16): 2453-2462.

22. Larson CN, Krantz BA, & Wilkinson KD (1998) Substrate Specificity of Deubiquitinating Enzymes: Ubiquitin C-Terminal Hydrolases. *Biochem*. 37: 3358-3368.

23. Akutsu M, Dikic I, & Bremm A (2016) Ubiquitin chain diversity at a glance. *J. Cell Sci*. 129: 875-880.